



CDF Note 10975

## Leptonic Asymmetry in $t\bar{t}$ Production

The CDF Collaboration  
URL <http://www-cdf.fnal.gov>  
(Dated: February 25, 2013)

### Abstract

We measure the asymmetry of the lepton in semileptonic  $t\bar{t}$  decays in the full Run II sample of  $9.4 \text{ fb}^{-1}$ . We develop a new technique to correct for the incomplete lepton acceptance and derive a parton-level asymmetry. The result of  $0.094^{+0.032}_{-0.029}$  is approximately  $2\sigma$  above the Standard Model NLO prediction of  $A_{\text{FB}}^{\text{lep}} = 0.036$ .

# 1 Introduction

## 1.1 The Lepton Asymmetry and $t\bar{t}$ Polarizations

Many proposed New Physics explanations for the top production asymmetry predict deviations in other observables. One such complementary measurement is the rapidity asymmetry of the lepton, defined as

$$A_{\text{FB}}^{\text{lep}} = \frac{N(qy_l > 0) - N(qy_l < 0)}{N(qy_l > 0) + N(qy_l < 0)} \quad (1)$$

where  $q$  is the lepton charge and  $y_l$  its lab-frame rapidity.

As a probe of top physics, the lab-frame lepton asymmetry has certain advantages. Isolated leptons are measured with very high precision, and the inclusive  $A_{\text{FB}}^{\text{lep}}$  depends only on the lepton's charge and direction. No jet-parton matching or kinematic reconstruction is necessary, and in fact the presence of energetic jets serves only to define the signal region.

There are two physical origins of  $A_{\text{FB}}^{\text{lep}}$ . First, the lepton inherits some of the asymmetry of its parent top. This is a straightforward kinematic effect - in the lab frame, the decay products are boosted by the top's momentum. If top production is asymmetric, this induces an asymmetry in all of the decay products as well. In addition, the lepton asymmetry is also sensitive to the polarization of the  $t\bar{t}$  system, which we will define as

$$P = \frac{N(t_R\bar{t}_R) - N(t_L\bar{t}_L)}{N(t_R\bar{t}_R) + N(t_L\bar{t}_L)} \quad (2)$$

where the beamline is taken as the spin quantization axis, and right-handed tops have spin vectors along  $+z$ .

Tops decay rapidly, with minimal interaction and before their spins can flip. The V-A coupling of the weak interaction then connects the directional distributions of the top decay products to the polarization of the tops at production. This has long been noted, along with the particular power of the lepton as an analyzer of top spin. One manifestation of this effect is a forward-backward asymmetry in the lepton from polarized tops.

Intuitively, this occurs as follows - consider a right-handed top pair  $t_R\bar{t}_R$  decaying semileptonically. In the rest frame of a top in a spin eigenstate, the direction of the lepton tends toward the direction of the top's spin (against for  $\bar{t}$ ). If the lepton originates with the  $\bar{t}$ , the resulting negative lepton is more often found in the backward region of the detector. On the other hand, if it is the  $t$  which decays leptonically, the positive lepton is more often in the forward region. Thus a  $t\bar{t}$  polarization causes an asymmetry of the lepton; an excess of  $t_R\bar{t}_R$  causes  $A_{\text{FB}}^{\text{lep}}$  to be more positive, and an excess of  $t_L\bar{t}_L$ , more negative.

This relationship between the top asymmetry, polarizations and the lepton asymmetry has been the subject of recent theoretical work in the context of New Physics explanations for the top asymmetry, such as [1] and [2].

The Standard Model predicts a small top production asymmetry and no polarization. However, several independent measurements (e.g. [3], [4]) indicate that the measured top production asymmetry significantly exceeds current Standard Model predictions. The presence of this asymmetry, along with the kinematic correlation between  $A_{\text{FB}}^{\text{lep}}$  and  $A_{\text{FB}}^{\Delta y}$ , suggests that a similar discrepancy should appear in the asymmetry of the lepton alone. In fact, previous measurements indicate that this is indeed the case - the inclusive lepton asymmetry has been measured by D0 at  $0.142 \pm 0.038$  in the semileptonic channel ([4]) and  $0.058 \pm 0.051 \pm 0.013$  in the dileptonic channel ([5]).

## 1.2 Overview of Measurement

The goal of this analysis is to produce a fully parton-level measurement of  $A_{\text{FB}}^{\text{lep}}$  in the lepton+jets channel. This will be accomplished as a several-step procedure, with measurements of the asymmetry produced at each stage of correction.

We will show that the charge-weighted lepton rapidity  $qy_l$  can be separated into a symmetric part  $\mathcal{S}(qy_l)$  and the functional dependence of the asymmetry  $\mathcal{A}(qy_l)$ . The symmetric part will be seen to be robust across different models, while  $\mathcal{A}(qy_l)$  encapsulates the variation from one model to the next and may be approximated by a simple mathematical form. We will fit this functional dependence in the data and use this in conjunction with the symmetric part taken from Monte Carlo to extract the production-level  $A_{\text{FB}}^{\text{lep}}$ .

Model	$A_{\text{FB}}^{\Delta y}$	$A_{\text{FB}}^{\text{lep}}$	Polarization	
ALPGEN	-0.000 (1)	+0.003 (1)	+0.009 (2)	LO Standard Model
POWHEG	+0.052 (0)	+0.024 (0)	+0.001 (1)	NLO Standard Model
Octet A	+0.156 (1)	+0.070 (2)	-0.005 (3)	LO unpolarized axigluon
Octet L	+0.121 (1)	-0.062 (1)	-0.290 (3)	LO left-handed axigluon
Octet R	+0.114 (2)	+0.149 (2)	+0.280 (3)	LO right-handed axigluon

Table 1: Generator-Level Monte Carlo asymmetries and polarizations.

### 1.3 Physics Models and Expected Asymmetry

In order to validate the technique of this analysis, we make use of several New Physics Monte Carlos in addition to Standard Model generators. We emphasize that the NP models are not to be interpreted as specific hypotheses which are to be falsified. Rather, they fill the more generic role of illuminating the manner in which a lepton asymmetry caused by various combinations of a top production asymmetry and polarization can be expected to manifest in the data.

All of the Monte Carlo models are showered with PYTHIA and processed with the full CDF detector simulation; the effects of showering are included in the generator-level plots. Simulated top events generated by ALPGEN and POWHEG represent the Standard Model at LO and NLO, respectively. Additionally, we use three Madgraph axigluon models which have been designed to have inclusive top asymmetries  $A_{\text{FB}}^{\Delta y}$  which are comparable to CDF lepton+jets data.

The two polarized models, Octet L and Octet R, are light (200GeV), wide (50GeV) axigluons. They are identical except that Octet L has a left-handed coupling (and therefore a negative  $P$ ) while Octet R has a right-handed coupling (positive  $P$ ). These are the polarized models of [1]. Octet A is a massive (2.0TeV), narrow axigluon with unpolarized couplings. All three New Physics models predict lepton and top asymmetries which deviate from the Standard Model, while largely preserving SM predictions in other variables.

The similar top asymmetries of the three axigluon models contrast the substantially different lepton asymmetries. The unpolarized Octet A has a lepton asymmetry which results only from the kinematic correlation with  $A_{\text{FB}}^{\Delta y}$ . In Octet R, the lepton asymmetry is enhanced by its right-handed polarization, whereas in Octet L the left-handed polarization overcomes the positive asymmetry from  $A_{\text{FB}}^{\Delta y}$  for a net negative value.

The expected lepton asymmetry in the context of the Standard Model has been investigated theoretically, e.g. [6], which incorporates both the next-to-leading-order QCD production mechanisms as well as electroweak interference effects. The authors calculate an inclusive Tevatron  $A_{\text{FB}}^{\text{lep}}$  at production level of  $0.036 \pm 0.002$ . We use this prediction to compare with our measured value.

The POWHEG Monte Carlo utilized in this analysis includes NLO QCD but not electroweak effects; the impact of the latter on  $A_{\text{FB}}^{\Delta y}$  has been estimated as a multiplicative factor of 1.26. If this holds for the lepton as well, the resulting prediction of POWHEG + EW at production level is  $A_{\text{FB}}^{\text{lep}} = 0.030$ . The difference from the calculation of [6] is primarily due to differing conventions as to whether the LO or NLO cross-section should be used in the denominator when calculating the asymmetry.

Both POWHEG and [6] make predictions for the top asymmetry which are well below that measured in the data. The question then arises as to what may be expected for  $A_{\text{FB}}^{\text{lep}}$  given the measured value of  $A_{\text{FB}}^{\Delta y}$ , in the context of purely SM decays. One approach is to simply examine Octet A; like the Standard Model, it predicts unpolarized top pairs and thus an  $A_{\text{FB}}^{\text{lep}}$  which is entirely due to the kinematic correlation with  $A_{\text{FB}}^{\Delta y}$ . As the top asymmetry is quite comparable with the CDF measurement, the predicted  $A_{\text{FB}}^{\text{lep}} = 0.070$  provides a reasonable expectation.

Another approach is to take the ratio  $(A_{\text{FB}}^{\Delta y}/A_{\text{FB}}^{\text{lep}})$ . This cancels both the multiplicative electroweak correction as well as the cross-section in the denominator. The ratio from POWHEG is 2.17; given the CDF measurement  $A_{\text{FB}}^{\Delta y} = 0.164$ , the expected asymmetry of the lepton would then be 0.076. Note that the unpolarized Octet A has a ratio of 2.23. The similarity to POWHEG suggests that a fixed ratio reasonably captures the effect of the kinematic correlation between the two asymmetries.

We conclude that, given the measured value of  $A_{\text{FB}}^{\Delta y}$  and assuming purely Standard Model decays, a reasonable expectation for  $A_{\text{FB}}^{\text{lep}}$  is 0.070 to 0.076.

## 2 Methodology

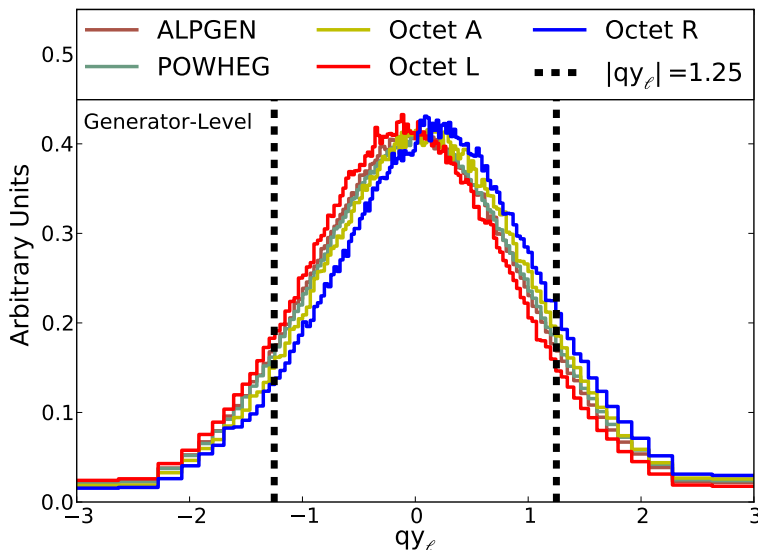


Figure 1: Generator-level  $qy_l$ . The vertical lines at  $|qy_l| = 1.25$  indicate the limits of the lepton acceptance.

The raw, measured asymmetry includes contributions from non- $t\bar{t}$  backgrounds and is further distorted by limited detector acceptance. Both of these effects must be accounted for in order to extract a parton-level result. The backgrounds may be easily accommodated by a bin-by-bin subtraction procedure (validated more thoroughly in Sec. 3.2). Correcting for acceptance, however, requires some care to accommodate the hard cutoff of  $y_l$  caused by the geometry of the detector.

The generator-level distributions of  $qy_l$  are shown in Figure 1. Vertical dotted lines indicate the limits of the lepton acceptance. The bulk of the  $qy_l$  distribution - about 80% of the total cross section - falls into the accepted region. However, the 20% of events which fall entirely outside the detector's range are generally the most asymmetric. The recovery of this contribution to the parton-level inclusive  $A_{\text{FB}}^{\text{lep}}$  necessarily relies on extrapolation of one form or another.

### 2.1 Rapidity Decomposition

To accomplish the extrapolation to the true production-level asymmetry, it will prove useful to decompose the signed rapidity distribution  $N(qy_l)$  into a symmetric part  $\mathcal{S}(qy_l)$  and the differential dependence of the asymmetry  $\mathcal{A}(qy_l)$ , defined as

$$\mathcal{S}(qy_l) = \frac{N(qy_l) + N(-qy_l)}{2} \quad (3a)$$

$$\mathcal{A}(qy_l) = \frac{N(qy_l) - N(-qy_l)}{N(qy_l) + N(-qy_l)} \quad (3b)$$

and taken to be defined in the range  $qy_l \geq 0$ . This decomposition is purely mathematical; the pair of functions  $\mathcal{S}(qy_l)$  and  $\mathcal{A}(qy_l)$  have exactly the same information content as  $N(qy_l)$ . They may therefore be inverted to recover the original distribution:

$$N(qy_l) = \mathcal{S}(qy_l) \times \begin{cases} 1 + \mathcal{A}(qy_l) & qy_l > 0 \\ 1 - \mathcal{A}(qy_l) & qy_l < 0 \end{cases} \quad (4)$$

This in turn may be integrated to recover the total number of forward or backward events:

$$N(qy_l > 0) = \int_0^{\infty} dqy_l [\mathcal{S}(qy_l) \times (1 + \mathcal{A}(qy_l))] \quad (5a)$$

$$N(qy_l < 0) = \int_0^{\infty} dqy_l [\mathcal{S}(qy_l) \times (1 - \mathcal{A}(qy_l))] \quad (5b)$$

which then yields the inclusive asymmetry, written in terms of  $\mathcal{S}(qy_l)$  and  $\mathcal{A}(qy_l)$ :

$$A_{FB}^{lep} = \frac{N(qy_l > 0) - N(qy_l < 0)}{N(qy_l > 0) + N(qy_l < 0)} \quad (6a)$$

$$= \frac{\int_0^{\infty} dqy_l [\mathcal{A}(qy_l) \times \mathcal{S}(qy_l)]}{\int_0^{\infty} dqy_l \mathcal{S}(qy_l)} \quad (6b)$$

## 2.2 $A_{FB}^{lep}$ in the $t\bar{t}$ Monte-Carlos; Extrapolation Procedure

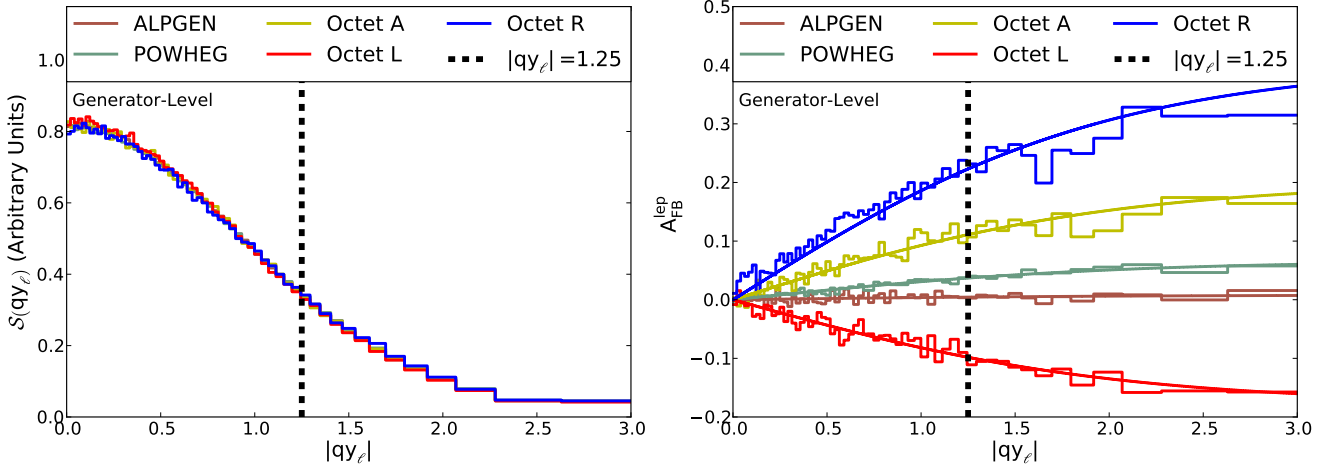


Figure 2: Generator-level  $qy_l$ , decomposed into the symmetric part (left) and asymmetry (right).

We next examine the Monte-Carlo models in terms of their symmetric and asymmetric parts. This is shown in Figure 3. Of note are two points:

1.  $\mathcal{S}(qy_l)$  is very similar across models. There is no apparent dependence on either the top production asymmetry or polarization.
2. The asymmetry rises steadily from zero at  $|qy_l| = 0$  before saturating well within the unsampled region.

The presumptive top events which cannot be seen by the detector are also the most asymmetric. At (roughly) 20% of the total cross-section, properly accounting for these events is essential to recovering the inclusive parton-level  $A_{FB}^{lep}$ . This requires an extrapolation procedure which is robust across models.

The decompositions of the Monte Carlos suggest a strategy for designing such a procedure. If  $\mathcal{A}(qy_l)$  can be parameterized such that its full dependence may be extracted from the measured asymmetry in the accepted region,

then the integral of equation 6 can be used to recover the parton-level asymmetry by integrating the measured dependence of  $\mathcal{A}(qy_l)$  against the predicted generator-level  $\mathcal{S}(qy_l)$  from Monte Carlo.

Fortunately,  $\mathcal{A}(qy_l)$  is generally well-described by the function

$$\mathcal{A}(qy_l) = a \tanh \left[ \frac{1}{2} qy_l \right] \quad (7)$$

This particular choice of parameterization is not expected to be truly model-independent. However, it accurately reproduces the dependence of the asymmetry on  $qy_l$  for the models discussed here. In particular, POWHEG is well-described, and it is therefore reasonable to expect this functional form to be reliable for any model with sufficiently SM-like kinematics.

Even with the full statistics of the Monte-Carlo samples, the fits generally have good  $\chi^2$ . In the presence of lepton asymmetries much larger than is seen in the data, such as the right-handed octet, the fits become less good. The fit to this model may be improved by the introduction of a second parameter (i.e. using the fit function  $a \tanh [b * qy_l]$ ). However, the introduction of a second parameter substantially increases the error due to statistics. In the next section we will show that the single-parameter fit is able to accurately recover the correct parton-level asymmetry even in the case of Octet R.

Explicitly then, the correction procedure from the measured  $qy_l$  to the parton-level lepton asymmetry is carried out in several stages:

- Bin-by-bin subtraction of expected backgrounds.
- Bin-by-bin acceptance corrections in the accepted region.
- Fit of  $\mathcal{A}(qy_l)$  in the accepted region.
- Integration of the fit  $\mathcal{A}(qy_l)$  with the Monte-Carlo  $\mathcal{S}(qy_l)$  to recover the inclusive  $A_{FB}^{lep}$ .

The binning of  $qy_l$  has been chosen so that POWHEG's predicted  $\mathcal{S}(qy_l)$  at the data level has equal statistics in each bin. The fit to  $\mathcal{A}(qy_l)$  is performed using the predicted bin centers from POWHEG. Once the fit parameter has been obtained from the background-subtracted data using this binning, the integration of Eqn. 6 is carried out numerically, using the 120-bin generator-level  $\mathcal{S}(qy_l)$  from POWHEG and the fit  $\mathcal{A}(qy_l)$  evaluated at POWHEG bin centers.

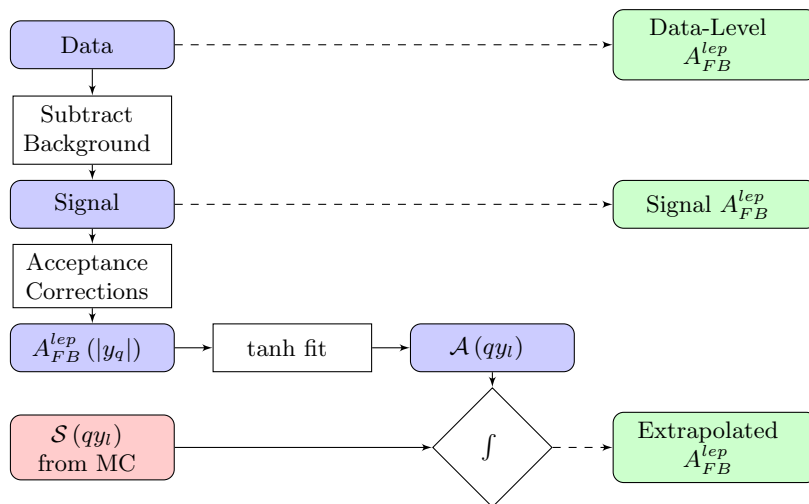


Figure 3: A graphical representation of the correction procedure.

CDF Run II Preliminary  $\int \mathcal{L} = 9.4/fb$

Signal Model	True $A_{\text{FB}}^{\text{lep}}$	Extrapolated $A_{\text{FB}}^{\text{lep}}$
ALPGEN	+0.003 (1)	-0.004
POWHEG	+0.024 (0)	+0.027
Octet A	+0.070 (1)	+0.069
Octet L	-0.062 (1)	-0.062
Octet R	+0.149 (2)	+0.155

Table 2: True Monte Carlo asymmetries compared to mean extrapolated results for 10,000 simulated experiments using the data statistics.

### 2.3 Validation

The efficacy of this correction procedure may be tested in a straightforward way. For each signal model, we generate a set of 10,000 simulated experiments with the statistics of the data. The extrapolation procedure is performed on each simulated experiment using bin-by-bin acceptance corrections derived from POWHEG. Differences between the generator-level asymmetry and the mean extrapolated asymmetry are indicative of possible biases.

The results of this process are shown in Table 2. The extrapolation procedure is generally successful at recovering the true asymmetry while introducing only minimal model-dependent biases. Deviations of the mean extrapolated result from the true asymmetry are uniformly below 0.01. In particular, the biases with POWHEG (NLO Standard Model) and Octet A (which has a similar  $A_{\text{FB}}^{\text{lep}}$  to the data) are very small.

## 3 Data Results

### 3.1 Event Selection and Sample Composition

We use the full CDF Run II dataset, corresponding to an integrated luminosity of  $9.4\text{fb}^{-1}$ . Lepton+jets candidate events are selected from high- $p_T$  electron or muon triggers. Additionally, we include events triggered by large missing  $E_T$  in which a high- $p_T$ , isolated muon is identified during offline reconstruction. Jets are reconstructed using a cone algorithm with cone radius  $R \equiv \sqrt{\eta^2 + \phi^2} = 0.4$ . The signal region is then defined by the following criteria:

- exactly 1 tight lepton,  $p_T > 20$  GeV
- Missing  $E_T > 20$  GeV
- Four or more jets with  $|\eta| < 2.0$ :
  - 3 jets with  $E_T > 20$  GeV
  - $\geq 1$  jet with  $E_T > 12$  GeV
  - $\geq 1$  “b-tagged” jet.
- $H_T \geq 220$

The veto of events with  $H_T < 220$  serves to reduce the contribution of non-W backgrounds while removing very little signal. The final sample for analysis consists of 3864 events, whose composition is estimated using the standard Method 2 calculation. The result is shown in Table 3.

CDF Run II Preliminary  $\int \mathcal{L} = 9.4/fb$

Process	Prediction	
Non-W	207	$\pm 86$
W+HF	481	$\pm 178$
W+LF	201	$\pm 72$
Single Top	67	$\pm 6$
Diboson	36	$\pm 4$
Z+jets	34	$\pm 5$
All Backgrounds	1026	$\pm 210$
$t\bar{t}$ 7.4pb	2750	$\pm 426$
Total Prediction	3776	$\pm 476$
Observed	3864	

Table 3: Sample composition as estimated by Method 2.

### 3.2 Asymmetries of the Backgrounds

Background processes are expected to contribute a nonzero asymmetry to the data-level result. The dominant background is W+jets, and both W+HF and W+LF are asymmetric. These processes have asymmetries arising from a combination of electroweak and PDF effects. Before examining the signal region, where the expected background will be subtracted from the data bin-by-bin, we wish to validate that the background and its asymmetry are properly modeled.

This is accomplished by examining events which otherwise meet the criteria of Sec. 3.1, but have exactly zero B-tagged jets. This “antitag” selection is orthogonal to the signal region while being kinematically very similar.  $qy_l$  in the antitag selection is shown in Figure 4.

The asymmetries of  $t\bar{t}$  and backgrounds in the antitag sample are summarized in Table 4. The predicted  $A_{\text{FB}}^{\text{lep}}$  is 0.062; the asymmetry in the data is  $0.076 \pm 0.011$ . This is already an acceptable level of agreement. However, approximately 20% of the antitag sample is still  $t\bar{t}$ . As a consistency check, we will anticipate the measurement of the background-subtracted asymmetry in the tagged region ( $A_{\text{FB}}^{\text{lep}} = 0.070$ ; see Section 3.3). If the  $t\bar{t}$  component is assumed to have this asymmetry, the predicted  $A_{\text{FB}}^{\text{lep}}$  in the antitag sample becomes 0.073, in excellent agreement with the measured value.

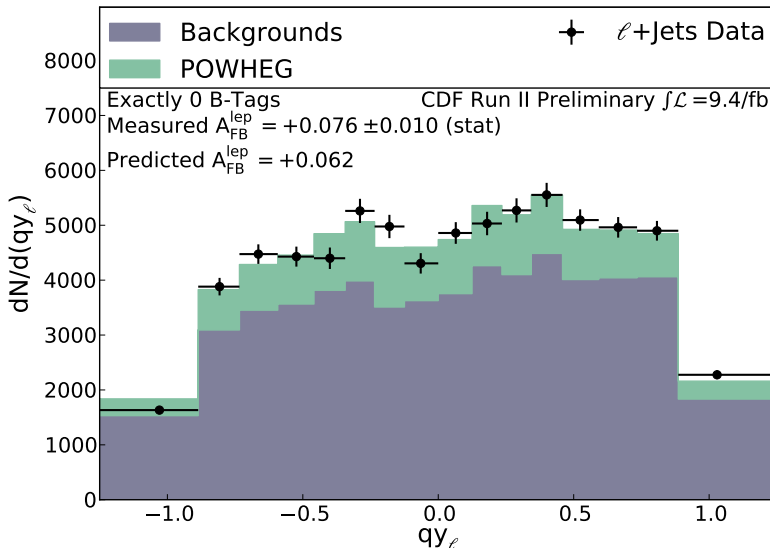


Figure 4:  $qy_l$  in the antitag control region.

CDF Run II Preliminary $\int \mathcal{L} = 9.4/\text{fb}$			
Asymmetry			
POWHEG	0.017		
Backgrounds	0.074		
POWHEG + Backgrounds	0.062		
*Signal + Backgrounds	0.073		
CDF Data	0.076	$\pm$	0.010

\*:  $A_{\text{FB}}^{\text{lep}}$  of  $t\bar{t}$  fixed to 0.070

Table 4: Comparison of the predicted and measured asymmetries in the antitag sample.

### 3.3 Signal Region; the Corrected $A_{\text{FB}}^{\text{lep}}$

We next examine the measured data while it is subject to each stage of the machinery of Section 2.2. The uncertainties quoted include both statistical and the appropriate systematic uncertainties, which will be described in further detail in the following section. The modeling of the CDF lepton+jets dataset has been extensively validated in several analyses. Here we reproduce only the  $p_T$  of the lepton (Figure 5) as this is the variable which is most relevant for the present purposes.

We now examine the measured distribution of  $qy_l$ , shown in Figure 6 (left). The inclusive asymmetry in the measured data is  $0.067 \pm 0.016$ , in some excess of the predicted value of 0.031. Figure 6 (right) shows the distribution of  $qy_l$  after backgrounds have been subtracted. The inclusive asymmetry is now  $0.070 \pm 0.022$ .

The background-subtracted  $qy_l$  is next decomposed into the corresponding  $\mathcal{S}(qy_l)$  and  $\mathcal{A}(qy_l)$ , shown in the two plots of Figure 7. It is seen that  $\mathcal{S}(qy_l)$  is in good agreement with the POWHEG expectation but that, as would be anticipated from the differing inclusive asymmetries, the measured  $A_{\text{FB}}^{\text{lep}}(qy_l)$  exceeds the predicted value in most bins.

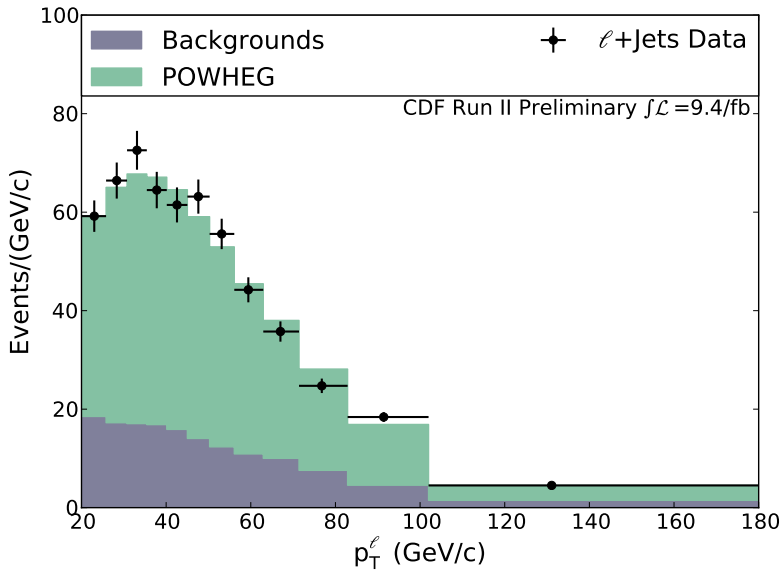


Figure 5: The  $p_T$  of the lepton.

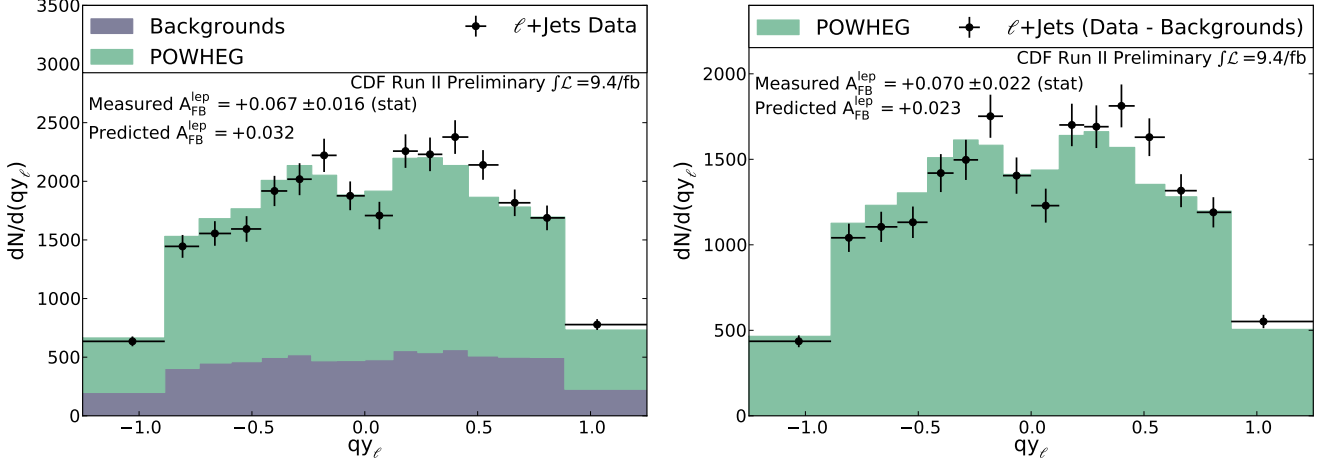


Figure 6: Left:  $qy_l$  in the data compared to POWHEG and the predicted background. Right:  $qy_l$  after background subtraction, compared to POWHEG

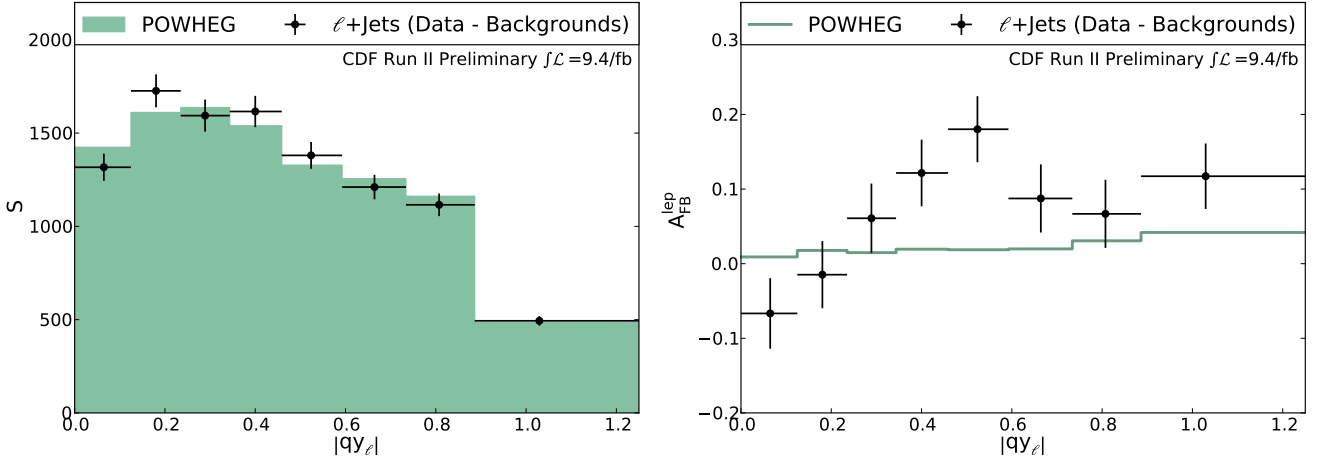


Figure 7:  $\mathcal{S}(qy_l)$  (left) and  $\mathcal{A}(qy_l)$  (right) after background-subtraction.

$A_{\text{FB}}^{\text{lep}}(qy_l)$  appears to display a degree of structure. It may be readily inferred that this is a somewhat unfortunate statistical fluctuation. As  $A_{\text{FB}}^{\text{lep}}(qy_l)$  is derived from  $qy_l$ , which is a continuous variable in any reasonable physical theory, its asymmetric part must necessarily approach zero as  $qy_l \rightarrow 0$ . Consequentially any deviations from this behavior are statistical in origin.

Next, POWHEG-based acceptance corrections are applied to the background-subtracted  $\mathcal{A}(qy_l)$  and the result is fit to Eqn. 7. The acceptance-corrected data, POWHEG prediction and fits to both are shown in 8. The parameter  $a$  takes the value  $0.266 \pm 0.079$  and the fit line reasonably captures the data. After performing the integration, the resulting inclusive asymmetry in the data is  $A_{\text{FB}}^{\text{lep}} = 0.094_{-0.029}^{+0.032}$ .

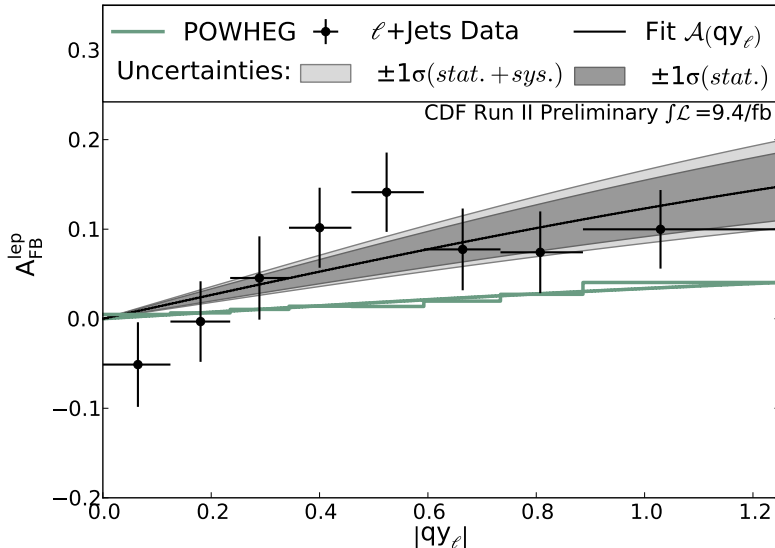


Figure 8:  $\mathcal{A}(qy_l)$  after acceptance-correction, with fits

### 3.4 Evaluation of Uncertainties

In the raw data, the uncertainty on the measured  $A_{\text{FB}}^{\text{lep}}$  is correctly due to statistics alone. However, each stage of correction imposes additional physical assumptions and, consequentially, introduces additional uncertainties into the measurement. Systematic uncertainties first enter when subtracting the background contributions. Backgrounds are removed statistically by subtracting the nominal value of each background component in each bin; that is, it is assumed that each background component has precisely the large-statistics shape of its Monte-Carlo prediction, scaled such that its normalization is the most probable value from Method 2.

To understand the impact of the backgrounds, we must incorporate both the effects of uncertain normalizations and finite bin statistics. This is most directly done by extending the method of Sec. 2.3 to include these effects. Each simulated experiment is now generated in the following manner: first, a normalization for each signal and background component is randomly generated from a Gaussian distribution, using the expected event count and error from Method II. Then, each bin of each normalized component is randomly varied according to Poisson statistics. The varied signal and varied backgrounds are then summed.

A set of 10,000 simulated experiments is generated using POWHEG as the signal model. Each is subject to the entirety of the correction procedure - the nominal background contribution is subtracted, acceptances are corrected bin-by-bin, and the result is extrapolated to a parton-level asymmetry. This incorporates into a single procedure the effects of data statistics, background statistics and uncertainties on the expected background normalizations. The variance of the resultant distribution of asymmetries is the uncertainty from these three effects in combination.

The signal model and its corresponding uncertainties enter only through the bin-by-bin acceptance corrections, which are Monte Carlo-derived. These types of uncertainties may be quantified by performing the correction procedure on the data using acceptances from alternate  $t\bar{t}$  Monte-Carlos. Uncertainties due to color reconnection, parton showering and jet energy scales are very small. This is unsurprising in a measurement which uses jets only to define the signal region. PDF uncertainties largely cancel when forming an asymmetry and so also have minimal impact.

The final two sources of systematic uncertainty relate to the modeling of effects due to radiation. The presence of radiated jets is strongly correlated with both the  $P_T$  of the  $t\bar{t}$  and the  $t\bar{t}$  asymmetry. Color predominantly flows from the initiating quark to the outgoing top (and from  $\bar{q}$  to  $\bar{t}$ ). A backward-going  $t\bar{t}$  pair is therefore more likely to radiate in order that color flow be conserved. Consequentially, backward-going events have a harder  $P_T$  spectrum, which leads to them being accepted with greater frequency. This asymmetry in the  $t\bar{t}$  acceptance in turn induces a similar asymmetry in the acceptance of the lepton.

The uncertainty due to the amount of radiation is quantified as the IFSR systematic. This effect is small.

The uncertainty on recoil modeling captures the impact of the dependence of the asymmetry on  $p_T^{\bar{t}}$ . There is poor agreement between various Monte Carlos on this dependence, and even between various tunes of a given Monte Carlo (see [7]). However, our nominal POWHEG model estimates the impact of this effect conservatively. We include a one-sided systematic uncertainty to reflect the fact that an improved understanding of this effect is likely to increase the measured value of the asymmetry.

Table 5 summarizes all of the considered uncertainties. The measurement is statistics-dominated, with the largest source of systematic uncertainty being the modeling of the backgrounds. The asymmetric recoil-modeling uncertainty follows, with the remainder of the uncertainties being very small.

CDF Run II Preliminary $\int \mathcal{L} = 9.4/fb$	
Source of Uncertainty	Value
Backgrounds	0.015
Recoil Modeling	+0.013 -0.000
Color Reconnection	0.0067
Parton Showering	0.0027
PDF	0.0025
JES	0.0022
IFSR	0.0018
Total Systematic	+0.021 -0.017
Data Statistics	0.024
Total Uncertainty	+0.032 -0.029

Table 5: Table of errors on the fully-extrapolated measurement.

### 3.5 Cross-Checks

To further check the validity of the inclusive  $A_{\text{FB}}^{\text{lep}}$ , we divide our sample into several subsamples which are expected to have the same inclusive asymmetries, summarized in Table 6.

First, two orthogonal subsamples are formed by partitioning by lepton type. At the data level, the asymmetry appears to be slightly greater for muons ( $0.081 \pm 0.022$ ) than electrons ( $0.050 \pm 0.024$ ). The difference is consistent with zero at about the  $1\sigma$  level. This difference is carried through each stage of correction, with similar levels of significance at each.

The sample is also partitioned by lepton charge. Here, at the data- and signal-level the difference between the two subsamples is nonzero at  $2\sigma$ . This moderates to  $1\sigma$  after the extrapolation procedure is performed. Again invoking the continuity of  $qy_l$ , this behavior is understood as a statistical fluctuation:  $A_{\text{FB}}^{\text{lep}}(qy_l)$  in the negative leptons contains negative-asymmetry bins near  $|qy_l| = 0$ . The fit, which by construction has  $\mathcal{A}(0) = 0$ , is insensitive to these bins. The moderation of the discrepancy in the extrapolated result is therefore a desired behavior.

CDF Run II Preliminary $\int \mathcal{L} = 9.4/fb$				
Sample	$N_{\text{events}}$	Data	Signal	Fully Extrapolated
Electrons	1788	$0.050 \pm 0.024$	$0.050 \pm 0.034$	$0.062^{+0.052}_{-0.049}$
Muons	2076	$0.081 \pm 0.022$	$0.087 \pm 0.029$	$0.119^{+0.039}_{-0.037}$
Positive	1884	$0.099 \pm 0.023$	$0.110 \pm 0.031$	$0.125^{+0.042}_{-0.041}$
Negative	1980	$0.036 \pm 0.022$	$0.034 \pm 0.031$	$0.063^{+0.045}_{-0.042}$
Inclusive	3864	$0.067 \pm 0.016$	$0.070 \pm 0.022$	$0.094^{+0.033}_{-0.030}$

Table 6: Table summarizing the resulting asymmetries when the sample is divided by either charge or lepton type. Also included is the inclusive result.

## 4 Conclusions

The parton-level lepton asymmetry has been measured to be  $A_{\text{FB}}^{\text{lep}} = 0.094^{+0.032}_{-0.029}$ . This exceeds the POWHEG prediction of 0.026 by roughly  $2.2\sigma$  and the QCD+EW prediction of  $0.036 \pm 0.002$  from [6] by  $2\sigma$ . However, the result is entirely consistent with the estimated  $0.070 - 0.076$  based on the measured inclusive  $A_{\text{FB}}^{\Delta y}$ .

The values of the inclusive  $A_{\text{FB}}^{\text{lep}}$  at each level of correction, along with errors incorporating the relevant systematic uncertainties, are summarized in comparison to POWHEG in Table 7.

CDF Run II Preliminary $\int \mathcal{L} = 9.4/\text{fb}$		
Correction Level	CDF Data	POWHEG
Data Only	$0.067 \pm 0.016$	0.032
Backgrounds Subtracted	$0.070 \pm 0.019 \pm 0.011$	0.023
Fully Extrapolated	$0.094 \pm 0.024^{+0.022}_{-0.017}$	0.027

Table 7: Measured asymmetries at each level of correction compared to the prediction of POWHEG and backgrounds.

## References

- [1] A. Falkowski, M. L. Mangano, A. Martin, G. Perez, and J. Winter, “Data driving the top quark forward–backward asymmetry with a lepton-based handle,” [arXiv:1212.4003 \[hep-ph\]](#).
- [2] E. L. Berger, Q.-H. Cao, C.-R. Chen, and H. Zhang, “Interpretations and Implications of the Top Quark Rapidity Asymmetries  $A_{\text{FB}}^t$  and  $A_{\text{FB}}^\ell$ ,” [arXiv:1209.4899 \[hep-ph\]](#).
- [3] **CDF** Collaboration, T. Aaltonen *et al.*, “Measurement of the top quark forward-backward production asymmetry and its dependence on event kinematic properties,” [arXiv:1211.1003 \[hep-ex\]](#).
- [4] **D0** Collaboration, D. Orbaker, “Measurement of the Forward-Backward Asymmetry in Fop-Antitop Quark Production in Proton-Antiproton Collisions,” [arXiv:1110.2062 \[hep-ex\]](#).
- [5] **D0** Collaboration, V. M. Abazov *et al.*, “Measurement of Leptonic Asymmetries and Top Quark Polarization in  $t\bar{t}$  Production,” [arXiv:1207.0364 \[hep-ex\]](#).
- [6] W. Bernreuther and Z.-G. Si, “Top quark and leptonic charge asymmetries for the Tevatron and LHC,” [arXiv:1205.6580 \[hep-ph\]](#).
- [7] J. Winter, P. Z. Skands, and B. R. Webber, “Monte Carlo event generators and the top quark forward–backward asymmetry,” [arXiv:1302.3164 \[hep-ph\]](#).